

# 1 Domain-Based Nucleic-Acid Minimum Free Energy: 2 Algorithmic Hardness and Parameterized Bounds

3 **Erik D. Demaine** ✉

4 Massachusetts Institute of Technology, USA

5 **Timothy Gomez** ✉

6 Massachusetts Institute of Technology, USA

7 **Elise Grizzell** ✉

8 University of Texas Rio Grande Valley, USA

9 **Markus Hecher** ✉

10 Massachusetts Institute of Technology, USA

11 **Jayson Lynch** ✉

12 Massachusetts Institute of Technology, USA

13 **Robert Schweller** ✉

14 University of Texas Rio Grande Valley, USA

15 **Ahmed Shalaby** ✉

16 Hamilton Institute, Department of Computer Science, Maynooth University, Ireland

17 **Damien Woods** ✉

18 Hamilton Institute, Department of Computer Science, Maynooth University, Ireland

## 19 — Abstract —

20 Molecular programmers and nanostructure engineers use domain-level design to abstract away  
21 messy DNA/RNA sequence, chemical and geometric details. Such domain-level abstractions are  
22 enforced by sequence design principles and provide a key principle that allows scaling up of complex  
23 multistranded DNA/RNA programs and structures. Determining the most favoured secondary  
24 structure, or Minimum Free Energy (MFE), of a set of strands, is typically studied at the sequence  
25 level but has seen limited domain-level work. We analyse the computational complexity of MFE for  
26 multistranded systems in a simple setting where we allow only 1 or 2 domains per strand. On the one  
27 hand, with 2-domain strands, we find that the MFE decision problem is NP-complete, even without  
28 pseudoknots, and requires exponential time algorithms assuming SAT does. On the other hand, in  
29 the simplest case of 1-domain strands there are efficient MFE algorithms for various binding modes.  
30 However, even in this single-domain case, MFE is P-hard for promiscuous binding, where one domain  
31 may bind to multiple as experimentally used by Nikitin [Nat Chem., 2023], which in turn implies  
32 that strands consisting of a single domain efficiently implement arbitrary Boolean circuits.

33 **2012 ACM Subject Classification** Theory of computation → Problems, reductions and completeness;  
34 Computer systems organization → Molecular computing

35 **Keywords and phrases** Domain-based DNA designs, minimum free energy, efficient algorithms,  
36 NP-hard, P-hard, NC, fixed-parameter tractable

37 **Digital Object Identifier** 10.4230/LIPIcs.CVIT.2016.23

38 **Funding** Elise Grizzell is supported in part by the U.S. Department of Education grant P200A120256.  
39 Markus Hecher is supported by the Austrian Science Fund grant J4656 and the Society for Re-  
40 search Funding NOE grant ExzF-0004. Robert Schweller is supported in part by National Science  
41 Foundation Grant CCF2329918. Damien Woods & Ahmed Shalaby are supported by the European  
42 Research Council (ERC, Active-DNA, No. 772766); European Innovation Council (EIC, DISCO,  
43 No. 101115422); and Science Foundation Ireland (SFI) Nos. 18/ERCS/5746 & 20/FFP-P/8843.

44 **Acknowledgements** We thank Jenny Diomidova, Marco Rodriguez, Tim Wylie for helpful discussions.



© Erik D. Demaine, Timothy Gomez, Elise Grizzell, Markus Hecher, Jayson Lynch, Robert Schweller,  
Ahmed Shalaby, Damien Woods;  
licensed under Creative Commons License CC-BY 4.0

42nd Conference on Very Important Topics (CVIT 2016).

Editors: John Q. Open and Joan R. Access; Article No. 23; pp. 23:1–23:24

Leibniz International Proceedings in Informatics



LIPICs Schloss Dagstuhl – Leibniz-Zentrum für Informatik, Dagstuhl Publishing, Germany

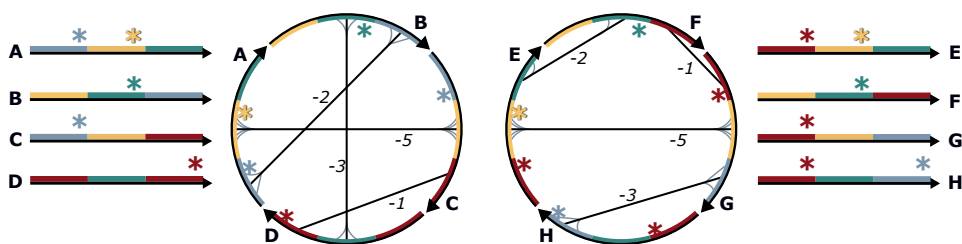
## 1 Introduction

Computational prediction of nucleic acid systems plays a crucial role in their design, analysis, and engineering. For a system of DNA or RNA strands, we typically desire prediction of likely secondary structures—strand bindings formed by base pairing—at thermodynamic equilibrium, but ignoring 3D geometry, strain, kinetics, and many other details, as shown in Figure 1. The most favored secondary structure(s) at chemical equilibrium are those with *minimum free energy* (MFE). To assign a probability to any secondary structure at equilibrium, the *partition function*, the sum of the Boltzmann-weighted energy of each secondary structure, is used as a normalization factor. Typically, the space of secondary structures is exponential in system size, hence, efficient algorithms to compute them may or may not exist. Decades of work have produced beautiful connections between secondary structure features and algorithmic efficiency (see Section 1.2), as well as predictive software packages [13, 28] for system analysis and design. For molecular programming, showing that a class of systems is algorithmically hard to predict often implies they embed algorithms and, hence, might make good candidates for molecular computers.

### 1.1 Background and justification for domain-level analysis

Algorithms for thermodynamic secondary structure prediction research traditionally focus on the *base-level* of abstraction: strings over the alphabet A, C, G, and T for DNA, or U instead of T for RNA. However, DNA/RNA nanostructures and molecular programs are typically designed at a higher *domain-level* of abstraction, better suited to large systems with complicated interactions, which led Shalaby, Thachuk, and Woods [44] to propose seeking *domain-level thermodynamic algorithms* for predictive analysis. A domain  $d$  is a substrand of DNA/RNA that is assumed to bind perfectly to its complement domain  $d^*$ , and to no other (Figure 1), although variations of this definition are also used. The main motivations are twofold: (i) good DNA/RNA sequence design, and good system design principles, can be used to enforce a domain-based abstraction, and (ii) even with that simplified abstraction, the energy landscape is typically of exponential size; hence, the task of finding clever and efficient algorithms is still required for domain-level prediction. In general, multistranded and pseudoknotted systems either have no known efficient algorithms or are NP-hard to predict at the base (nucleotide) [1, 29, 30, 12] and/or domain [12] level. However, despite the lack of algorithmic thermodynamic prediction, multistranded and pseudoknotted domain-based nanostructure designs are some of the most successful to date, including DNA origami [40], RNA origami [22], and single/double-stranded tile systems [52, 54, 53, 18]. Clearly, the design process for these systems does not rely solely on full algorithmic prediction of secondary structure thermodynamics, but rather alternative methods, such as decomposing the system into smaller unpseudoknotted pieces [54, 18, 22] or by intuition-driven whiteboard sketches—all at the domain level. These successful experimental implementations give evidence for the benefits of domain-based design. Still, nevertheless, the lack of theoretical underpinning suggests a need for exclusively domain-based thermodynamic prediction algorithms [44] to continue along the journey of scale-up and complexification.

Since domains are merely a coarse-grained abstraction of DNA bases, the accuracy of domain-level models typically depends on good-quality DNA sequence design [54, 19, 48, 37, 55, 51], or on choosing biologically-sourced/random sequences with good enough properties [40]. Interestingly, domain-level design creates new challenges for thermodynamic prediction algorithms. Domain-level systems, like base-level systems, as noted above, tend to have exponentially large secondary structure spaces, meaning the existence of efficient



■ **Figure 1** (Left): Domain-level system with 4 DNA strands having 3 domains each; codomains are indicated by \*. (Middle-left): Example polymer graph of the strands showing domains bound a binding function  $\delta$  with negative integer number strengths, e.g.  $\delta(\text{green}, \text{green}^*) = -3$  (indicated both by numbers and by count of short grey/black curves attaching to a domain). (Right): Another domain-level system with four strands, having a maximally bound polymer graph with no crossings, showing that these strands have an unpsseudoknotted MFE secondary structure.

91 (polynomial time) prediction algorithms may not be obvious. Further, domain-level systems  
 92 may have an arbitrary number of domain types (base-level systems have only 4), as well as  
 93 non-complementary (promiscuous) binding, meaning that the number of potential interactions  
 94 in a system grows quickly with increasing system size.

## 95 1.2 Previous work on MFE and partition function

96 At the DNA base-level, for any  $n$ -strand connected secondary structure  $s$ , the free energy  
 97  $\Delta G(s) = \sum_{l \in s} \Delta G(l) + (n-1)\Delta G^{\text{assoc}} + k_B T \log_e R$ , where  $k_B$  is Boltzmann's constant in  
 98 units of kcal/(mol · K) and  $T$  is temperature in Kelvin (K). In particular, this free energy  
 99 includes the sum of the empirically-obtained free energies  $\Delta G(l)$  of the constituent loops [13]  
 100 of  $s$ , which are secondary structure features such as stack loops, hairpin loops, and others [41].  
 101  $\Delta G^{\text{assoc}} > 0$  is an entropic association penalty for bringing strands together, and there is an  
 102  $R$ -fold rotational symmetry penalty that is strictly positive for secondary structures with  
 103 repeated strands that have several so-called rotational symmetries [13, 45]. The MFE of a set  
 104  $\Omega$  of secondary structures is simply  $\min_{s \in \Omega} \Delta G(s)$ , and the partition function is the number  
 105  $Q = \sum_{s \in \Omega} e^{-\Delta G(s)/k_B T}$ . We use  $Q$  to define the probability of any secondary structure  $s$  at  
 106 equilibrium:  $p(s) = (e^{-\Delta G(s)/k_B T})/Q$ .

107 At the domain-level, as in [44], we let  $\Delta G(s) = \sum_{(d,e) \in B} \Delta G(d,e) + (n-1)\Delta G^{\text{assoc}}$ ,  
 108 i.e. without any  $R$ -fold symmetry correction where  $B$  is the set of bonds of  $s$  and where  
 109  $\Delta G(d,e)$  is the binding strength of domains  $d, e$  (defined more formally in Section 2).

### 110 Known algorithmic results

111 Almost all prior algorithmic work is at the DNA/RNA base-level, recent domain-level  
 112 exceptions being [12, 44]. Single-stranded unpsseudoknotted systems of length  $L$  bases have  
 113 polynomial time  $\mathcal{O}(L^4)$ <sup>1</sup>. In 1990, McCaskill [32] showed dynamic programming efficiently  
 114 calculates single-stranded partition function in polynomial time  $\mathcal{O}(L^4)$ , allowing computation  
 115 of probabilities at equilibrium.

<sup>1</sup> We note that in the literature [13, 56, 12, 32] the polynomial is sometimes written to the power 3 (i.e.  $\mathcal{O}(L^3)$  for single stranded and  $\mathcal{O}(L^3(|S|-1)!$  for multistranded). This reduction in overhead comes from changing the standard energy model by putting some restrictions on the size of interior loops [13], or by enforcing certain mild conditions on the energy parameters for the interior loops [31, 25]

116 **Multistranded systems.** For systems with a constant number of strands ( $|\mathcal{S}| = \mathcal{O}(1)$ )  
 117 strands, independent of total number of bases  $L$ ), also unpsuedoknotted, Dirks et al. [13], gave  
 118 a polynomial time,  $\mathcal{O}(L^4(|\mathcal{S}|-1)!)$ , partition function algorithm, leaving MFE open. Recently,  
 119 Shalaby and Woods [45] gave an  $\mathcal{O}(L^4(|\mathcal{S}|-1)!)$  time algorithm for MFE in the same setting.  
 120 In terms of computational complexity both of these problems are Fixed Parameter Tractable  
 121 (FPT) with respect to strand count. For multi-stranded systems with a non-constant number  
 122 of strands  $|\mathcal{S}|$  and domain length  $L$ , Condon, Hajiaghayi, and Thachuk [12] showed a negative  
 123 result: it is NP-complete [33] to predict MFE unpsuedoknotted secondary structure(s), and  
 124 even hard to approximate. They reduce from a variant of 3-dimensional matching (3DM) [20],  
 125 with their result holding whether or not rotational symmetries are accounted for.

126 **Pseudoknots.** If we allow pseudoknots, there are as-of-yet unsolved modeling considerations:  
 127 energy models are challenging to formulate due to the increased significance of geometric  
 128 issues and tertiary interactions [13]. For simple energy models that allow pseudoknots, it  
 129 is known that MFE prediction is NP-complete even for a single strand [1, 29, 30]. But,  
 130 efficient dynamic programming algorithms exist for restricted classes of pseudoknots, for  
 131 both MFE [39, 49, 11, 27, 38] and partition function [14, 15].

132 **Domain-level.** Two papers with domain-level algorithmic results are: Condon, Hajiaghayi,  
 133 and Thachuk [12] showing multistranded MFE is NP-complete, and Shalaby, Thachuk,  
 134 and Woods [44] giving a polynomial-time MFE algorithm for a subclass of multistranded  
 135 systems—both papers utilize a long scaffold strand in different ways to give essentially  
 136 opposite results.

### 137 1.3 Our Contributions

138 Our results, summarized in Table 1, mainly focus on MFE for multi-stranded systems with  
 139 1 or 2 domains per strand. Such few-domain systems are experimentally well-motivated:  
 140 for example, SST systems [52] have only four domains per strand yet are capable of reas-  
 141 onably complicated computation [54], as are other tile systems [18, 43, 53, 4]. Nikitin [35]  
 142 uses 1-domain promiscuous-binding to run depth-2 Boolean circuits, and there are strand  
 143 displacement systems that compute using two [10] to a few [46, 55, 47] domains per strand.

144 We begin, in Section 2, with formal domain-based definitions of DNA secondary structures.  
 145 In Section 3 we show there are small, 1 or 2 strand, systems with only 2 domains per strand  
 146 that have pseudoknotted MFE structures (useful for later results). In our **first main result**,  
 147 we show the simple-sounding case of 2-domain strands has NP-hard MFE (Theorem 14,  
 148 Section 4). This uses the straightforward setting of perfectly complementary domains with  
 149 all-equal binding strengths and improves the NP-hardness result of Condon, Hajiaghayi,  
 150 and Thachuk [12], which required a long  $\mathcal{O}(m)$ -domain strand (for a 3DM instance with  
 151  $m$  triples). Both of these hardness results are then leveraged to give parameterized lower  
 152 bounds on  $|\mathcal{S}|$  and  $L$ , assuming the exponential time hypothesis (ETH) that there is no  
 153 subexponential time algorithm for SAT.

154 We then investigate systems of strands with one domain (Section 5). Our **second main**  
 155 **result**, Theorem 18, states that 1-domain systems, with promiscuous but bipartite binding  
 156 and multiple strengths, are P-hard to predict (and hence likely unparallizable [33]). Moreover,  
 157 this problem can be viewed as a natural generalization of the classic Edge Weighted Matching  
 158 problem in which the vertex set is given as a multi-set with binary encoded counts. Showing  
 159 that the Edge Weighted Matching problem is P-hard is a long-standing open problem [24].  
 160 Thus, the P-hardness of MFE for single-domain strands could provide important insights  
 161 into this classic problem.

162 Theorem 19 gives an MFE algorithm running in time polynomial in the number of

163 strands  $|\mathcal{S}|$ . Theorem 20 shows bipartite (domains and codomains) unit-strength binding  
 164 is even easier, giving an  $\mathcal{O}(|\Lambda|^3)$  time algorithm, i.e., an algorithm that is polynomial-time  
 165 even when strand counts are provided in binary. Finally, for complementary binding, MFE  
 166 is easier again as we have a sequential  $\mathcal{O}(|\Lambda|)$  time one (Theorem 21), and a  $\mathcal{O}(\log |\mathcal{S}|)$ -time  
 167 parallel algorithm (Theorem 22). The parallel algorithm puts this problem in the class  
 168 NC [33], which taken together with Theorem 18 implies that promiscuous binding, multiset  
 169 encoding, or both are needed for efficient simulation of sequential computation.

170 Our final result, Theorem 23, shows that the counting version of the free energy problem  
 171 (that we call #FE) is #P-complete even for 1-domain strands and bipartite binding. While  
 172 this doesn't show hardness for computing the partition function (PF), these problems are  
 173 related since an efficient algorithm for #FE can be used to compute PF in  $\text{P}^{\#\text{P}} = \text{P}^{\text{PP}}$  when  
 174 the range of energy levels is polynomial. This relates PF to the counting hierarchy (CH) [50].  
 175 We also note that many of our results on 1-domain strands are reductions to or from the  
 176 matching problem, the partition function of which, on regular graphs, has been investigated  
 177 before [9, 6].

## 178 1.4 Future Work

179 For 1-domain strands, the main open question is to give an upper bound on the power of  
 180 promiscuous binding with counts encoded in binary—shown here to be P-hard (Theorem 18).  
 181 We believe this can be solved using b-matchings and thus P-complete<sup>2</sup>. Another interesting  
 182 problem is whether the P-hardness result holds under further restrictions. If so, this must  
 183 still take advantage of promiscuous binding or exponential strand count due to the NC result,  
 184 Theorem 22.

185 What is the best run time for a FPT algorithm for MFE for strands with  $L$  domains  
 186 which runs in time  $2^{\mathcal{O}(|\mathcal{S}|)} \cdot L^{\mathcal{O}(1)}$  that accounts for rotational symmetry? We note that two  
 187 recent papers give (a) an algorithm that handles rotational symmetry in the Turner/nearest  
 188 neighbour model [45] (which could be ported to the domain model we use here, but with  
 189 likely increase in run time due to the increase from 4 bases to  $|\Lambda|$  domains), and (b) a singly-  
 190 exponential algorithm that does not handle rotational symmetry [7] running in  $\mathcal{O}(3^{|\mathcal{S}|} \cdot L^3)$   
 191 time, making our lower bound tight up to ETH. The next interesting parameters to study  
 192 are the number of domains  $|\Lambda|$  or the number of strand types  $|\Sigma|$ .

## 193 2 Domain Based DNA Model

194 In this section, we discuss our DNA model and problems of interest.

195 ► **Definition 1** (Domains, Codomain, and Strands). *A domain is a pair (label, dir) where*  
 196 *label is a unique id usually represented by a letter and  $\text{dir} \in \{\rightarrow, \leftarrow\}$  is a direction. The*  
 197 *codomain of domain  $a$  is the domain with the same label and opposite direction, denoted by*  
 198  *$a^*$ . Let  $\Lambda$  be a set of domains, a strand  $\sigma \in \Sigma$  is a sequence of domains all with the same*  
 199 *direction (the strand is said to have that direction) denoted  $\overrightarrow{ab}$  (for a 2-domain strand) and*  
 200 *sometimes called 5' to 3' order. However, when it is clear that all domains have the same*  
 201 *direction, we denote these as tuples  $(a, b)$ .  $\mathcal{S}$  denotes a multiset of strands, and  $\Sigma = \text{Supp}(\mathcal{S})$*   
 202 *denotes the support, or unique strand types, of  $\mathcal{S}$ .*

<sup>2</sup> This was pointed out after submission by Marco Rodriguez.

#Domains	Binding Type	Run Time Bounds	Complexity
$L$	Complementary & unit strength	UB: $\mathcal{O}( \Lambda L^3 \mathcal{S} ^4 \cdot ( \mathcal{S}  - 1)!)$ (Thm. 15), LBs: $2^{\Omega(\min( \mathcal{S} , L))}$ (Thm. 17)	NP-C [12]
2	Complementary & unit strength	UB: $\mathcal{O}( \Lambda  \mathcal{S} ^4 \cdot ( \mathcal{S}  - 1)!)$ (Thm. 15), LB: $2^{\Omega( \mathcal{S} )}$ (Thm. 16)	NP-C (Thm. 14)
1	Promiscuous	UB: $\mathcal{O}( \mathcal{S} ^4)$ (Thm. 19)	P <sup>†</sup> (Thm. 19), P-hard (Thm.18)
1	Bipartite unit strength	UB: $\mathcal{O}( \Lambda ^3 \log  \mathcal{S} )$ (Thm. 20)	P (Thm. 20)
1	Complementary	UB: $\mathcal{O}( \Lambda  \log  \mathcal{S} )$ (Thm. 21)	NC <sup>†</sup> (Thm. 22)

■ **Table 1** Results for unpseudoknotted domain-level MFE. Upper bounds (UBs) are for a deterministic sequential algorithm with worst-case running time shown. All lower bounds (LBs) assume **ETH**. <sup>†</sup>Result holds for input **encoded in unary** and does not hold for input **encoded in binary**.

203 ► **Definition 2** (Binding Function/Strength). *The binding function  $\delta : \Lambda^2 \rightarrow \{0, -1, -2, \dots\}$*   
 204 *gives the binding strength between any two domains (more negative is more favorable).*

205 The previous definition assumes negative *integer* binding strengths between domains. We  
 206 note that in the literature, more general rationals or reals (typically negative) are used for  
 207 ‘stack’ energies [41], but our use of integers simplifies giving precise bounds on energy ranges.

208 We use the following definitions to classify the different types of binding functions:

- 209 ■ **Unit Strength:** For all  $a, b \in \Lambda$ ,  $\delta(a, b) \in \{0, -1\}$ , i.e. non-0 binding strengths are equal.
- 210 ■ **Bipartite:** The domains can be partitioned into disjoint sets  $\Lambda = \Lambda_D \cup \Lambda_C$ , referred to  
 211 as *domains* and *codomains*, such that for any two  $a, b$  in the same set  $\delta(a, b) = 0$
- 212 ■ **Complementary:** We say a binding function is complementary if it is bipartite and  
 213 there exists a perfect matching, meaning for all domains  $a \in \Lambda_D$ , there exists  $a^* \in \Lambda_C$ ,  
 214 such that  $\delta(a, a^*) < 0$ , and for all other pairs the binding strength is zero.
- 215 ■ **Promiscuous:** Any non-complementary binding function is said to be promiscuous  
 216 (which may be bipartite or not).

217 ► **Definition 3** (Domain-level strand system). *A domain-level strand system  $D$ , or simply*  
 218 *system, is a multiset  $\mathcal{S}$  of strands over support strand set  $\Sigma = \text{Supp}(\mathcal{S})$  and a binding func-*  
 219 *tion  $\delta$ .*

220 ► **Definition 4** (Domain-level secondary structure  $s$ ). *For any domain-level strand system, a*  
 221 *domain-level secondary structure, or simply secondary structure,  $s$ , is a set of domain pairs*  
 222 *(hydrogen bonds, or simply bonds) respecting the binding function where no domain belongs*  
 223 *to two pairs. Each domain is specified by a strand identifier and a position on that strand.*  
 224 *For example,  $(i_p, j_q)$  denotes domain  $i$  of strand  $p$  binds to domain  $j$  of strand  $q$  such that*  
 225  *$\delta(i_p, j_q) \neq 0$ .*

226 Each secondary structure consists of one or more complexes:

227 ► **Definition 5** (Complex). *A complex is a domain-pair connected domain-level secondary*  
 228 *structure. Here, we also assume that each strand is connected: i.e. within each strand,*  
 229 *consecutive domain pairs are connected (in their direction, i.e. 5' to 3' order).*

230 A **polymer graph** for a secondary structure  $s$  of a system  $D$  with multiset of strands  $\Sigma$ ,  
 231 and ordering of those strands  $\pi$ , is constructed by drawing them in  $\pi$ -order in the 5' to 3'  
 232 direction around the circumference of a circle where: (i) the domains along each strand are  
 233 assumed to be connected, in 5' to 3' order (by their *covalent bonds*), (ii) there is a **nick** (gap,

234 i.e. no edge) between two adjacent strands and (iii) there is a chord connecting each domain  
 235 pair (*hydrogen bond, or bond*) of  $s$ . Examples are shown in Figures 1–3. Let  $|\mathcal{S}|$  denote the  
 236 total number of strands (cardinality) in the multiset  $\mathcal{S}$ . The set of circular permutations,  $\Pi$ ,  
 237 of these  $|\mathcal{S}|$  strands contains  $(|\mathcal{S}| - 1)!$  distinct circular permutations since cyclic permutations  
 238 change the location of the strands on the circle without affecting their relative orderings  
 239 (e.g., for three interacting strands  $\{A, B, C\}$ ,  $\Pi = \{ABC, ACB\}$  since the orderings  $ABC$ ,  
 240  $BCA$ , and  $CAB$  are the same on a circle) [8]. Each circular permutation  $\pi \in \Pi$  there has a  
 241 distinct polymer graph.

242 ► **Definition 6** (Pseudoknot-free, or unpseudoknotted, secondary structure). *For any secondary*  
 243 *structure  $s$ , we call  $s$  pseudoknot-free, or unpseudoknotted, if  $s$  has at least one circular*  
 244 *permutation  $\pi \in \Pi$  yielding a planar polymer graph (no crossing domain-pair edges), otherwise*  
 245 *we call  $s$  pseudoknotted.*

246 In the following domain-based definition of free energy, we do not consider the entropic  
 247 penalty due to rotational symmetry when there are repeated strands [13, 45].

248 ► **Definition 7** (Free energy  $\Delta G(s)$ ). *The free energy, or simply energy, of a  $|\mathcal{S}|$ -strand,*  
 249  *$k$ -complex domain-level secondary structure  $s$  is  $\Delta G(s) = \sum_{(a,b) \in s} \delta(a,b) + (|\mathcal{S}| - k)\Delta G^{\text{assoc}}$ .*

250 ► **Definition 8** (MFE secondary structure). *For any domain-level strand system  $D$ , an*  
 251 *MFE secondary structure is any unpseudoknotted secondary structure  $s$  such that  $\Delta G(s) =$*   
 252  *$\min_{s' \in \Omega} \Delta G(s')$ , where  $\Omega$  is the set of all unpseudoknotted secondary structures of  $D$ .*

253 An example of two polymer graphs, one pseudoknotted and the other unpseudoknotted,  
 254 with their associated strands, can be found in Figure 1.

## 255 2.1 Problems and Parameterized Complexity

256 In computational complexity theory, it is useful to formalize problems as yes/no decision  
 257 problems. In this paper, we are mainly concerned with the MFE decision problem, which asks  
 258 whether the MFE of a system is below some threshold. This decision problem is in the class  
 259 NP since one can give a secondary structure as a certificate and quickly, in polynomial time,  
 260 compute its free energy and output yes/no depending on whether it is below the threshold.

261 ► **Definition 9** (Minimum Free Energy (MFE) decision problem). *Given a domain-level strand*  
 262 *system and a number  $k$ , does there exist a secondary structure  $s$  such that  $\Delta G(s) \leq k$ ?*

263 We assume the input to the MFE decision problem includes a **multiset** of strands (plus the  
 264 binding function) where each strand is given as  $(\sigma_i, c_i)$  where  $\sigma_i \in \Sigma$  is the strand type and  
 265  $c_i$  is an integer representing the number of copies of  $\sigma_i$  in the multiset  $\mathcal{S}$ . Due to this, we  
 266 say an algorithm that runs in time  $|\mathcal{S}|^{\mathcal{O}(1)}$  runs in **pseudopolynomial time**, since it runs  
 267 in time polynomial in the cardinality of the multiset  $\mathcal{S}$ , i.e. the number of strands in the  
 268 system, but not in the total input length (in bits). In some theorem statements, we refer  
 269 to counts being **encoded in unary**, meaning the strands are given as a set with repeated  
 270 strands written multiple times. This allows us to make claims about membership for “small”  
 271 values. The goal of these statements is to show that hardness must make use of the multiset  
 272 encoding, which has in other contexts been stated as Strong vs Weak NP-hardness [21].<sup>3</sup>

<sup>3</sup> A famous example of this is the partition problem [20] where we’re given  $n$  integers and a value  $T$  and we want to know if there exists a subset of the number which sums to exactly  $T$ . This problem is solvable in time  $\mathcal{O}(nT)$  but is NP-hard.

273 For our algorithms, we define our computational model to be **deterministic sequential**  
 274 **RAM** machines with constant time memory access unless stated otherwise. We allow for  
 275 constant time arithmetic of  $\log_2 n$ -bit numbers for input size  $n$ . This assumption does not  
 276 speed up the run time of our algorithms by more than a factor of  $\mathcal{O}(\log n)$ .

277 We also consider the problem of counting the number of structures of free energy  $k$ .

278 ► **Definition 10** (Counting Structures with Free Energy (#FE)). *Given a domain-level strand*  
 279 *system and a value  $k$ , how many secondary structures  $s$  exist with  $\Delta G(s) = k$ ?*

280 **Fixed-Parameter Tractable (FPT)** Algorithms run "fast" for instances with small  
 281 parameters. For example, an algorithm that has a runtime of  $f(k) \cdot n^{\mathcal{O}(1)}$  is said to be FPT  
 282 in  $k$ . The **Exponential Time Hypothesis (ETH)** claims that there does not exist a  $2^{o(n)}$   
 283 algorithm for SAT on  $n$  variables. This hypothesis establishes a technique for hardness and  
 284 lower bounds by assuming ETH is true. By designing reductions that preserve parameters,  
 285 we can achieve lower bounds for other problems such as MFE. These lower bounds are in the  
 286 form of "There does not exist an algorithm that runs in time  $2^{o(k)} \cdot n^{\mathcal{O}(1)}$ ".

### 287 **3 Pseudoknots**

288 Pseudoknots are surprisingly simple to form or avoid with short (few-domain) strands.  
 289 We begin by establishing a condition for 2-domain strands that prevents the formation of  
 290 pseudoknots. Then, we present short strands that have pseudoknotted minimum free energy  
 291 (MFE) structures.

#### 292 **3.1 Pseudoknotted and Unpseudoknotted Systems**

293 We define sided strands and show these cannot form pseudoknots. We use sided strands  
 294 in the next section to avoid forming pseudoknots in our reductions. We show that this  
 295 limit is somewhat tight in the sense relaxing this requirement allows for extremely simple  
 296 pseudoknots to form in the domain-level model.

297 ► **Definition 11** (Sided 2-domain strands). *A set of bipartite 2-domain strands is sided if*  
 298 *every strand has the form  $(a, b^*)$  with  $a \in \Lambda_D$  and  $b^* \in \Lambda_C$*

299 ► **Theorem 12.** *Any secondary structure  $s$  containing only  $(\leq 2)$ -domain "sided" strands is*  
 300 *unpseudoknotted, i.e. there is a strand order for  $s$  without crossings in the polymer graph.*

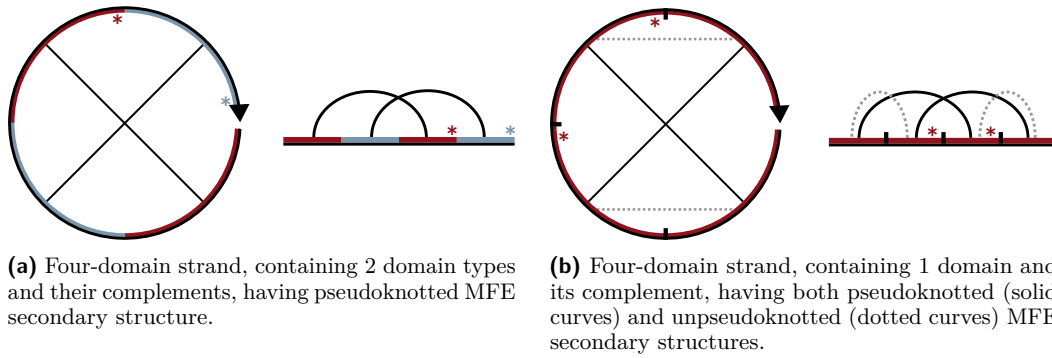
301 **Proof.** Recall that a secondary structure  $s$  includes a set of strands and their bonds. For  
 302 any  $s$ , create an ordering on strands as follows. Select some sided strand  $(a, b^*)$  and add it  
 303 to the drawing. If  $b^*$  is bound to another strand  $(b, c^*)$  in  $s$  then add that strand next in the  
 304 ordering. Repeat this process until either (1) you reach a strand  $(d, a^*)$  where  $a^*$  is bound  
 305 to  $a$  on the initial strand or (2) you reach a strand  $(d, z)$  where  $z$  is not bound to anything.  
 306 Each adjacent strand added to the drawing has a bond drawn to its neighbor strand without  
 307 crossing anything. If we end in case (1) we have built a cycle and can draw the new bond  
 308 above all the others without crossing. If there still exist strands that are not yet added to  
 309 the ordering, select one to add to the cycle then continue. ◀

310 Pseudoknots appear in MFE secondary structures, even for one or two strands:

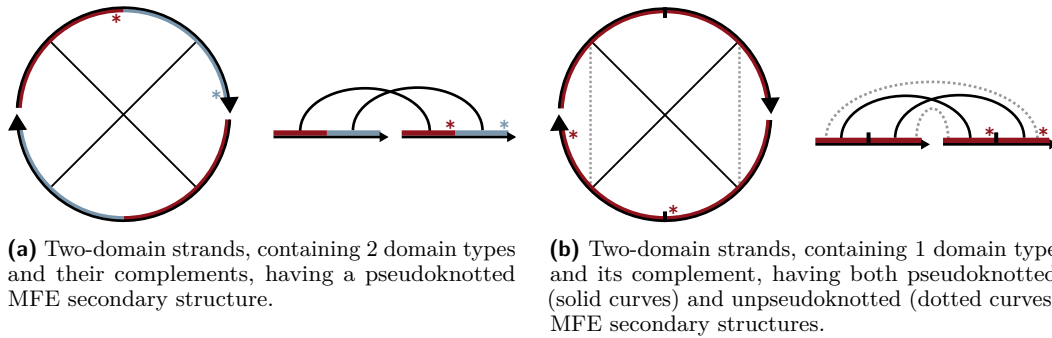
311 ► **Theorem 13.** *There exists a domain-level strand system with pseudoknotted MFE secondary*  
 312 *structure  $s$ , with as few as 1 or 2 strands in the strand multiset  $\mathcal{S}$ . There are several scenarios:*

313 ■  $\mathcal{S} = \{((a, b, a^*, b^*), 1)\}$  and  $s$  is the unique MFE secondary structure





■ **Figure 2** Single-stranded systems with only a few domains and pseudoknotted MFE structures.



■ **Figure 3** Double-stranded systems with only a few domains and pseudoknotted MFE structures.

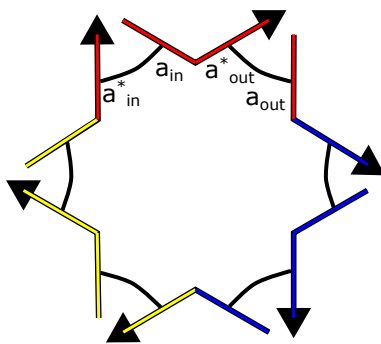
- 314 ■  $S = \{((a, a^*, a^*, a), 1)\}$  and  $s$  is not a unique MFE secondary structure
- 315 ■  $S = \{((a, b), 1), ((a^*, b^*), 1)\}$  and  $s$  is the unique MFE secondary structure
- 316 ■  $S = \{((a, a), 1), ((a^*, a^*), 1)\}$  and  $s$  is not a unique MFE secondary structure

317 **Proof.** MFE secondary structures are in Figures 2 and 3. The single strand  $(a, b, a^*, b^*)$  is  
 318 pseudoknotted since the only way to have two bonds is via a crossing. The strand  $(a, a^*, a, a^*)$   
 319 has two polymer graphs with 2 bonds, both with equal energy, although one has no crossings  
 320 and the other does. The same proof can be seen for the cases with 2 strands. We note there  
 321 is only one ordering for the case of 2 strands as the ordering is circular. ◀

## 322 4 Strands with 2 Domains

323 In this section, we show that the MFE problem is NP-hard even when strands contain only  
 324 2 domains. We show NP-hardness by reducing from the Directed 3-Cycle Cover problem  
 325 with the promise that there are no doubly covered edges. This variant of 3-cycle cover asks:  
 326 for a given graph, which does not have any 2-cycles, whether we can find a vertex-disjoint  
 327 set of (directed) 3-cycles of the graph, such that all vertices are covered (occur in a 3-cycle).  
 328 Theorem 24 in Appendix A shows this case of the cycle cover problem is NP-hard. We  
 329 provide helper lemmas in the Appendix as well.

330 We start with the reduction from 3-cycle cover to the MFE problem in Theorem 14. This  
 331 reduction holds even for unpseudoknotted structures from Theorem 12 as our strands are  
 332 sided. Turning to parameterized complexity we describe the ETH based lower bounds, which  
 333 follow from our reduction and the reduction from previous work [12]. We also cover the  
 334 relation between these lower bounds and recent FPT algorithms shown in [45].



■ **Figure 4** A complex representing a 3-cycle is built from 3 vertex strands and 3 edge strands. Each vertex strand is of a different color.

### 335 The Reduction

336 We now reduce the Directed 3-Cycle Cover with no 2-Cycles problem to MFE. Let  $G = (V, E)$   
 337 be a given input directed graph with no 2-cycles. In this reduction, we create vertex strands  
 338 and edge strands. Each cycle of our cover is represented by its own complex.

339 **Domains.** For each vertex  $v \in V$  we create four domains,  $v_{in}, v_{in}^*, v_{out}, v_{out}^*$ . Domains  
 340 marked with  $*$  are codomains in  $\Lambda_C$ . The binding function is complementary and unit  
 341 strength.

342 **Strands.** For each vertex  $v$  we create a strand  $\overrightarrow{v_{in}v_{out}^*}$ . For each edge  $(a, b) \in E$  we  
 343 create a strand  $\overrightarrow{a_{out}b_{in}^*}$ .

344 **Complexes.** The intuition behind this construction is that each complex will represent  
 345 a valid path in  $G$ . Each secondary structure will then be a set of vertex disjoint paths. A  
 346 cycle is represented by a complex that has no free domains. A 3-cycle is shown in Figure 4.  
 347 We refer to the secondary structure in which all vertices are contained in (disjoint) 3-cycle  
 348 complexes (if such a configuration exists) as a 3-cycle secondary structure.

349 ► **Theorem 14.** *MFE of domain-level strand systems with 2-domain strands is NP-Complete.*  
 350 *It remains NP-complete when restricted to sided strands, complementary binding, unit strength*  
 351 *bonds, and single strand multiplicities.*

352 **Proof.** To show this, we provide an energy value  $k$  such that the MFE instance will have a  
 353 secondary structure of energy less or equal to  $k$  if and only if the graph  $G$  has a 3-cycle cover,  
 354 which implies NP-hardness by Theorem 24. Assume  $0 < \Delta G^{\text{assoc}} < 1$  and set  $k$  as follows:

$$k = \Delta G(s) = -2n + \left(\frac{5n}{3}\right) \Delta G^{\text{assoc}}.$$

355 Now, suppose  $G$  has a 3-cycle cover, which implies the 3-cycle secondary structure exists.  
 356 We know from Lemma 27 that this secondary structure  $s$  has  $2n$  bonds and  $(m - \frac{2n}{3})$   
 357 complexes, which implies  $s$  has energy:

$$\Delta G(s) = -2n + \left((n + m) - \left(m - \frac{2n}{3}\right)\right) \Delta G^{\text{assoc}} = -2n + \left(\frac{5n}{3}\right) \Delta G^{\text{assoc}} = k.$$

358 Therefore, such an MFE instance is a *yes* instance.

359 Now, suppose there is no 3-cycle cover. This means there is no 3-cycle secondary  
 360 structure. By Lemma 29, we know the minimum energy secondary structure must have  $2n$

361 bonds. Therefore, Lemma 28 implies that this structure must have fewer than  $(m - \frac{2n}{3})$   
 362 complexes, which implies it has energy strictly greater than  $k$ , i.e. this MFE instance is a *no*  
 363 instance. ◀

## 364 4.1 Parameterized Complexity

365 Beyond just hardness, we look at the MFE problem from a more fine-grained (parameterized)  
 366 perspective. Precisely, we parameterize on the strand length  $L$  and number  $|\mathcal{S}|$  of strands.  
 367 We start by generalizing a known FPT algorithm [36] with respect to  $|\mathcal{S}|$  to the domain-level  
 368 model. Unfortunately, in general we can not avoid an exponential-time algorithm (unless  
 369 the exponential time hypothesis fails) even for short strands  $L \geq 2$ . For fixed length 2 case  
 370 we then give the conditional lower bound in Theorem 16 proven by our reduction. For the  
 371 general case, we then give a combined lower bound in Theorem 17 based on the minimum of  
 372  $|\mathcal{S}|$  and  $L$ . This shows the limits of FPT algorithms with respect to  $|\mathcal{S}|$ .

## 373 4.2 FPT Upper Bound

374 We prove this for bipartite unit-strength binding to compare against Theorem 14 and [12].  
 375 However these techniques should generalize incurring only a polynomial run time increase.

376 ▶ **Theorem 15.** *MFE of domain-level strand systems with bipartite unit strength and*  
 377 *pseudoknot free secondary structures is computed in time  $\mathcal{O}(|\Lambda|L^3|\mathcal{S}|^4 \cdot (|\mathcal{S}| - 1)!)$  for  $|\mathcal{S}|$*   
 378 *strands of max length  $L$  over  $|\Lambda|$  domain types.*

379 **Proof.** Consider a circular permutation  $\pi$  (out of  $(|\mathcal{S}| - 1)!$  circular permutations) of the  
 380 system strands. We use an extension algorithm of the single stranded maximum matching  
 381 model algorithm [36]. The main extension is to include the multi-stranded case and the  
 382 entropic penalties associated with it. The resulting recursion equation for the minimum  
 383 free energy,  $M_{i,j}$ , of a subsequence  $Y$  of the ordering  $\pi$ , where  $Y$  runs the  $i$ th domain to  $j$   
 384 domain, is as follows:

$$385 \quad M(i, j) = \min \begin{cases} M(i, k - 1) + M(k + 1, j - 1) - 1 + \mathcal{I}(j, k)\Delta G^{\text{assoc}} \\ M(i, j - 1) \end{cases}$$

386 Where  $\mathcal{I}(j, k)$  is an indicator variable such that  $\mathcal{I}(j, k) = 1$  iff both domains  $j$  and  $k$   
 387 belong to two different complexes. As we have two cases, (1) domain  $j$  does not form any  
 388 domain-pair, or (2) domain  $j$  forms a domain-pair with some domain  $k \in \{i, i + 1, \dots, j - 1\}$ .  
 389 If domain  $j$  and  $k$  were belonging to two different complexes, then entropic penalty  $\Delta G^{\text{assoc}}$   
 390 must be added, as they forming a domain-pair and hence reducing the number of complexes  
 391 by one.

392 The algorithm will require a square matrix  $M(i, j)$  as [36], but we augment each entry  
 393 with a list of complexes that are formed in the minimum free energy structure within the  
 394 the subsequence  $(i, j)$ , such that each complex is a set of strands. Note that the size of all  
 395 complexes at each entry can not exceed the number of strands. The value  $\mathcal{I}(j, k)$  equals zero  
 396 iff the two strands of domains  $j$  and  $k$  belong to the same complex (no entropic reduction)  
 397 of the minimum free energy structure of the subsequence  $(k + 1, j - 1)$  (found in the entry  
 398 of  $M(k + 1, j - 1)$ ), otherwise  $\mathcal{I}(j, k)$  equals one (applying entropic penalty). We ensure  
 399 choosing the appropriate  $k$  that guarantees that that domains  $(j + 1)$  and  $(i - 1)$  will be in  
 400 the same complex if possible with augmenting this boolean value also (to ensure the least  
 401 entropic penalty in future iterations), otherwise any  $k$  that minimize  $M(i, j)$  works, which

## 23:12 Domain-Based Nucleic-Acid Minimum Free Energy

402 requires extra  $\mathcal{O}(|\mathcal{S}|)$  time. Computing the augmented list of complexes at each entry follows  
403 directly based on  $k$ , and determining the value of  $\mathcal{I}(j, k)$  takes then a constant time.

404 The time complexity of [36] is  $\mathcal{O}(N^3)$  where  $N$  is the number of bases, in our case  
405  $N = \mathcal{O}(L|\mathcal{S}|)$  domains. So, the time complexity of our algorithm will be  $\mathcal{O}(|\Lambda|L^3|\mathcal{S}|^4 \cdot (|\mathcal{S}|-1)!)$   
406 considering the overhead of choosing the appropriate  $k$  that directly helps in determining  
407 the value of  $\mathcal{I}(j, k)$ , and the look up for the binding interaction of domains, and considering  
408 the whole possible circular permutations. ◀

### 409 Fixed Domain Length

410 For our reduction, we derive a lower bound of  $2^{\Omega(|\mathcal{S}|)}$ , even for  $L = 2$ , assuming ETH. This  
411 implies there does not exist a FPT algorithm with respect to strand length. In this case  
412 Theorem 15 gives a run time of  $\mathcal{O}(|\Lambda||\mathcal{S}|^4 \cdot (|\mathcal{S}|-1)!) = \mathcal{O}(|\Lambda|) \cdot 2^{\mathcal{O}(|\mathcal{S}|\log|\mathcal{S}|)}$ .

413 ▶ **Theorem 16.** *MFE for domain-level strand systems with 2-domain strands requires time*  
414  *$2^{\Omega(|\mathcal{S}|)}$ , unless ETH fails. This holds even when restricted to sided strands, complementary*  
415 *binding, and unit strength bonds.*

416 **Proof.** The result follows from Lemma 25 and Theorem 14. Observe that thereby  $|\mathcal{S}|$   
417 corresponds to  $n + m$ , where  $n$  is the number of variables and  $m$  is the number of edges.  
418 However, by using the so-called sparsification result [26] in advance, we can ensure both  
419 these terms are linear, giving the desired bound. Sparsification allows us to take advantage  
420 of the “trade-off” between the two parameters to achieve lower bounds on both  $n$  and  $m$ . ◀

### 421 Strand Count

422 For FPT algorithms we fix  $|\mathcal{S}|$  to be some constant and consider  $f(|\mathcal{S}|) \cdot \text{poly}(L, |\Lambda|)$  to be  
423 efficient. We are interested in getting a more precise estimate of  $f(|\mathcal{S}|)$ . Theorem 15 has a  
424 exponential factor of  $\mathcal{O}((|\mathcal{S}|-1)!)$ . Without fixing strand length we show a lower bound  
425 of  $2^{\Omega(|\mathcal{S}|)}$  (Theorem 17) using the 3DM reduction given by [12].

426 ▶ **Theorem 17.** *MFE for domain-level strand systems with  $L$ -domain strands requires time*  
427  *$2^{\Omega(\min(|\mathcal{S}|, L))}$ , unless ETH fails.*

428 **Proof.** In the reduction by Condon, Hajiaghayi, and Thachuk [12], from 3DM, the long  
429 strand length  $m$  was equal to the number of sets in the 3DM proof. The number of strands  
430 in the system is  $\mathcal{O}(n)$ . If we apply sparsification [26] first, we may assume that  $m + n$  is  
431 linear in  $n$ . Consequently, the result directly follows from a  $2^{\Omega(m)}$  ETH lower bound for  
432 3DM [3]. ◀

## 433 5 Strands with 1 domain

434 In this section we first prove that MFE is P-hard for strands with only a single domain, and  
435 promiscuous binding (Theorem 18), by giving a simulation of Boolean circuits. The proof  
436 crucially uses multiple copies of each strand type. Then, we give three algorithms, the first  
437 of which (Theorem 19) shows that if the MFE problem is encoded in unary it is solvable in  
438 time  $\mathcal{O}(|\mathcal{S}|^4)$ , even with promiscuous binding. We then provide an algorithm for bipartite  
439 unit strength binding which runs in time  $\mathcal{O}(|\Lambda|^3)$ , Theorem 20. Our last algorithm shows  
440 easiness for complementary binding (Theorems 21 and 22).

## 441 5.1 P-hardness of single-domain promiscuous binding: Simulating 442 Boolean circuits

443 In this section, we show P-hardness for MFE with single-domain strands by showing that  
444 computing MFE requires simulating/evaluating Boolean circuits. As shown later in the proof  
445 of Theorem 19, MFE with single-strand domains can be thought of as a weighted matching  
446 problem. Since weighted matching is not known to be P-hard [24], our P-hardness MFE  
447 result might be of independent interest as it shows P-hardness for a natural generalization of  
448 weighted matching in which the vertex set is given as a multi-set with binary encoded counts.  
449 **Some background on Boolean circuits and P-completeness.** The circuit value problem  
450 (CVP) asks: given a Boolean circuit and its input, is the output 1? The problem is in P,  
451 as any circuit can be evaluated in time polynomial in circuit size and input length, and is  
452 P-hard since circuits efficiently simulate Turing machines, and that simulation (or reduction)  
453 can be encoded in one of the classes conjectured to be strictly in P (e.g. L, or  $NC^1$ ; or with  
454 a little more work using a class known to be strictly contained in P, e.g.  $FAC^0$ ). In 1977,  
455 Goldschlager [23] showed that monotone circuits, i.e. those that use only AND, OR, and  
456 input gates, are P-complete to predict. The trick is to use dual-rail logic: run one monotone  
457 circuit  $c$  on the input  $x \in \{0, 1\}^*$  and on its bitwise complement  $\bar{x}$ , run a ‘complementary’  
458 monotone circuit denoted  $c'$  such that  $c'(\bar{x}) = c(x)$ . Since the dual-rail circuit is entirely  
459 monotone, a non-monotone reduction is used to convert  $x$  to  $\bar{x}$ . Even stronger, Theorem 6.2.5  
460 of Greenlaw and Ruzzo [24], states that the following problem is P-complete: Synchronous,  
461 Alternating, Monotone Circuit-Value Problem with fanout exactly 2. Here, *synchronous*  
462 means that the circuit gates are organized into layers, where gates in layer  $i$  only take inputs  
463 from layer  $i - 1$ . Every non-input gate has *fanout exactly 2*. Together with the property  
464 of being synchronous, this implies each non-input layer has the same number of gates (for  
465 decision problems, we only care about a single output bit of the circuit. Hence, there will be  
466 some redundant gates in the circuit). *Alternating* means that odd layers contain only OR  
467 gates and even layers only AND gates, except layer 0, which has input gates.

468 In a recent experimental paper, Nikitin [35] shows how to simulate 2 layer Boolean circuits  
469 by cleverly using what he terms “strand commutation” which is a form of promiscuous DNA  
470 strand binding using a mixture of mismatching and matching base pairs. Taking inspiration,  
471 we generalize his technique in several ways: (a) giving a proof that works for circuits of  
472 arbitrary depth, (b) having a fanin-2, fanout-2 gate design that has almost the same  $\Delta G$ ,  
473 except for multiples of some  $\epsilon$ , for each of the 4 possible input bit pairs, (c) an overall circuit  
474 design for which the MFE is guaranteed to sit in an easily defined energy interval that is a  
475 simple function of circuit size and depth. Together, these properties are leveraged to establish  
476 the P-hardness of the MFE problem for single-domain systems. We note that this theorem  
477 holds in a generalization of the TBN model [16], where we allow promiscuous binding.

478 ► **Theorem 18.** *MFE of domain-level strand systems with 1-domain strands, promiscuous*  
479 *(but bipartite) binding, and exponential strand counts, is P-hard to predict, under logspace*  
480 *reductions.*

481 **Proof.** Let  $C$  be any synchronous, alternating, monotone Boolean circuit where every gate  
482 has fanout exactly 2, and in particular,  $C$  uses only AND (fanin 2), OR (fanin 2), and input  
483 (fanin 0) gates. As discussed above, the problem of predicting families of such circuits is  
484 P-hard (Theorem 6.2.5 of [24]).

485 Let  $c$  be a copy of  $C$  and let  $c'$  be the dual circuit of  $c$  constructed as follows: For every  
486 non-input gate  $g$  in  $c$ , there is  $g'$  in  $c'$  where  $g'$  is OR iff  $g$  is AND, and vice-versa, and the  
487 input of  $c'$  is the bit-flipped input of  $c$ , with the wiring diagram being the same for both

488 circuits (this is the standard dual-rail technique). Thus, for all gates  $g: g(x_1, x_2) = \overline{g'(\overline{x_1}, \overline{x_2})}$   
 489 where  $x_1, x_2 \in \{0, 1\}$ , and for the entire circuit  $c(x) = \overline{c'(\overline{x})}$  where  $\overline{x}$  denotes the bitwise  
 490 complement of  $x \in \{0, 1\}^*$ .

491 **Simulating a single gate  $G$ .** Intuitively, we wish to simulate each gate  $G$  in  $C$  using a  
 492 strand gadget such that each gate in a layer has *almost* the same strand-gadget-MFE no  
 493 matter which of the four input bit pairs  $G$  receives. Suppose  $C$  consists of a single gate  $G$ .

494 Suppose further that  $G$  is an AND gate. We claim that  $G$  is simulated by the 1-domain  
 495 strand gadget in Figure 8 that operates by simultaneously simulating the corresponding AND  
 496 ( $g$ ) in  $c$  and OR ( $g'$ ) in  $c'$ . By simulate, we mean that (i) strands  $out_1$  and  $out_2$  are present  
 497 in the MFE structure iff  $g(x_1, x_2) = 1$ , and (ii) that the gadget MFE lies in a real-valued  
 498 interval to be defined later. Property (i) follows by a careful analysis of the binding energies  
 499  $\delta_1 < \dots < \delta_5$  (Figure 8), which are designed such that: input strands bind with strength  $\delta_1$   
 500 breaking up  $\delta_2$  bonds, freeing black strands to bind to the intermediate gadget green strands  
 501 with  $\delta_3$  (or grey-green with  $\delta_3 + \epsilon$ , for some  $\epsilon > 0$  to be defined later), with excess black  
 502 strands binding to brown/orange with  $\delta_4$  to release pink outputs that were bound with  $\delta_5$ .

503 If  $G$  is an OR gate, the same scheme is used except (a) all input bits and strands are  
 504 flipped, and (b) the output comes from the OR component of Figure 8. Else,  $G$  is an input  
 505 gate that is simulated by a single input strand type if  $G = 1$  and zero strands if  $G = 0$ .

506 **Gate at an arbitrary layer of an arbitrary  $C$ .** Now let  $C$  be of arbitrary size. Let  $d$   
 507 be the depth of  $C$  and hence also of  $c$  and  $c'$  (we define the depth  $d$  to be the number of  
 508 non-input layers),  $s$  be the size (including input gates), and  $h = (s - |x|)/d$  be the height of  
 509  $C$  (or number of gates per non-input layer—since every gate has equal fanin and fanout of 2  
 510 (except for input gates), all non-input layers have the same number of gates  $h$ , and the input  
 511 layer has  $2h$  gates). The input layer is  $\ell = 0$ .

512 Let  $g$ , in layer  $\ell > 0$ , be any non-input gate in  $c$ , and let  $in_1$  be any one of its 2 input  
 513 wires and let  $out_1$  be any one of its 2 output wires. The wire  $in_1$  has an associated, unique  
 514 strand type  $\sigma_{in_1}$ . The number of input strands (the count) of type  $\sigma_{in_1}$  is  $|\sigma_{in_1}| = 2(2^{d-\ell})$  if  
 515 the input bit is 1 and 0 if the input bit is 0. The number of output strands (the count) of  
 516 type  $\sigma_{out_1}$  is  $|\sigma_{out_1}| = 2^{d-\ell}$ , if the output bit is 1 and 0 if the output is bit 0.

517 As shown in Figure 9, each gate has 11 strand types. We define gate  $g$  to have a total  
 518 count of  $26 \times 2^{d-\ell}$  strands, which can be seen as a multi-set of 11 strand types with repetition  
 519 numbers shown in Figure 9.

520 We claim that the MFE, denoted by  $k_g^{(a,b)}$ , of any gate gadget  $g$  with any input bits  
 521  $(a, b)$ ,  $a, b \in \{0, 1\}$ , has value in the negative integer range  $[k_\ell, k_\ell + 2^{d-\ell+1}\epsilon]$  where  $k_\ell =$   
 522  $2^{d-\ell}(4\delta_1 + 4\delta_2 + 2\delta_3 + 2\delta_4 + 2\delta_5)$ . We will prove that claim by induction on  $(d - \ell)$ . For the  
 523 base step,  $(\ell = d)$ , our construction in Figure 8 represents any final-layer gate  $g_{\ell,i} = g_{d,i}$ :  
 524 specifically, the bottom of each of four Figure 8 panels shows that  $k_{g_{d,i}}^{(a,b)}$  lies in the claimed  
 525 interval, for each of the four cases of  $(a, b) \in \{0, 1\}^2$ . Suppose that the claim is valid for  
 526 any gate  $g_{\ell,i}$  in layer  $\ell$  such that  $(d - \ell) > 0$  giving the following induction hypothesis:  
 527  $k_{g_{\ell,i}}^{(a,b)} \in [k_\ell, k_\ell + 2^{d-\ell+1}\epsilon]$ . Now, for any gate at the non-input layer  $(\ell - 1)$ , and from the  
 528 recursive nature of our construction (Figure 10), leading to an exponential blow-up from right-  
 529 to-left (towards the input), gives  $k_{\ell-1} = 2k_\ell$ , which implies that  $k_{g_{\ell-1}}^{(a,b)} \in [k_{\ell-1}, k_{\ell-1} + 2^{d-\ell+2}\epsilon]$ .

530 Let  $E = \sum_{\ell \in \{1, 2, \dots, d\}} h 2^{d-\ell+1}\epsilon$  the sum of all  $\epsilon$ 's. Let  $\epsilon = +1$ . We will add an extra  
 531 gadget, called the output gadget, which consists of a single strand that binds to the strand  
 532 type  $out_1$  of the single circuit output (final) gate, with binding strength  $\delta_F = -E - 1$ . Also,  
 533 let  $\delta_5^F$  be the  $\delta_5$  value for the circuit's final output gate: we set  $\delta_5^F = \delta_F - 1$ , and for each  
 534 gate set  $\delta_5 = \delta_4 + 1 = \delta_3 + 3 = \delta_2 + 4 = \delta_1 + 5$  to satisfy the inequality shown in Figure 8  
 535 and have integer-only strengths (a definition that propagates binding strengths back through

536 circuit gadgets, from output back to inputs).

537 **Formula for MFE.** We next claim that  $c$  (and thus  $C$ ) accepts iff  $\text{MFE} < \sum_{\ell \in \{1,2,\dots,d\}} k_\ell h$ .  
 538 To see this note that *without the output gadget* (i.e. ignoring  $\delta_F$ ) the MFE is in the negative  
 539 integer interval:

$$540 \quad \left[ \sum_{\ell \in \{1,2,\dots,d\}} k_\ell h, E + \sum_{\ell \in \{1,2,\dots,d\}} h k_\ell \right] \quad (1)$$

541 but since  $\delta_F < -E$ , we know that the MFE including the output gadget (i.e. including  $\delta_F$ )  
 542 lies below the interval in (1) and this will happen iff circuit  $C$  accepts its input  $x$ .

543 We claim the reduction is computable by deterministic logarithmic space Turing ma-  
 544 chine [34, 2] that takes input  $C, x$ : We assume the circuit is described in a standard way as  
 545 a string [5]. The circuit height  $h$  and depth  $d$  are easily computed in logspace (e.g. count the  
 546 number of gates that take input from the first layer to give  $h$ , and divide that into circuit  
 547 size to get  $d$ ). Each gate description includes 11 strand types, unique to the gate (Figures 8  
 548 and 9), which are straightforward functions of the gate name. For each strand type, its  
 549 count is a function of circuit depth and gate layer (Figure 9) that uses multiplication and  
 550 exponentiation, on binary numbers of  $O(|x|^{O(1)})$  bits (these numbers are powers of 2 so could  
 551 be written using  $O(\log |x|)$  bits, although that is not required here since logspace machines  
 552 can output polynomial-sized words). Likewise for the MFE threshold value:  $\sum_{\ell \in \{1,2,\dots,d\}} k_\ell h$ .  
 553 The binding function (Figure 8), for any pair of strands, is a simple formula of the depth.  
 554 All gates at layer  $l$  have the same binding function as they do not interact with each other.  
 555 Hence, at layer  $l$ , the binding strength  $\delta_1 = -(E + 1 + 6d)$ , and  $\delta_2, \dots, \delta_5$  values follow  
 556 directly as described above. This value of  $\delta_1$  guarantees that  $\delta_F = -E - 1$  ( $E$  is a power  
 557 of 2, so all  $\delta$ 's could be written using  $O(\log |x|)$  bits). ◀

## 558 5.2 Polynomial-time algorithms for simulating 1-domain systems

559 ▶ **Theorem 19.** *MFE of domain-level strand systems with 1-domain strands is solvable in*  
 560  *$\mathcal{O}(|\mathcal{S}|^4)$ , even for promiscuous binding functions. With unary encoded counts, this problem*  
 561 *is in  $P$ .*

562 **Proof.** Create a graph  $G$  where each node is a strand. Multiple strands of the same type  
 563 have multiple nodes. For every pair of nodes representing strands with domains  $a$  and  $b$ , add  
 564 an edge with weight  $(-1)\delta(a, b) - \Delta G^{\text{assoc}}$  (to make weights positive).

565 Each weight is then the contribution of a complex to the energy. Since we are computing  
 566 a matching, each strand will be used once. The graph size will be  $|\mathcal{S}|$  and the upper bound  
 567 on the number of edges is  $|\mathcal{S}|^2$ . Since MAX weight matching has a  $\mathcal{O}(V^2 E)$  time algorithm,  
 568 this gives a  $\mathcal{O}(|\mathcal{S}|^4)$  algorithm for MFE. ◀

### 569 Bipartite Unit Strength

570 ▶ **Theorem 20.** *MFE of domain-level strand systems with 1-domain strands, bipartite binding,*  
 571 *and unit-strength bonds, is in  $P$  and solvable in  $\mathcal{O}(|\Lambda|^3 \log |\mathcal{S}|)$ , even for promiscuous binding*  
 572 *functions.*

573 **Proof.** We solve this by reducing it to the max-flow problem. Let  $A = a_1, a_2, \dots, a_n$  and  
 574  $B = b_1, b_2, \dots, b_m$  denote the bipartite partition for the domains of a given MFE instance,  
 575 and let  $c(x)$  denote the strand count for a given domain  $x$  (i.e. the number of strands with  
 576 domain  $x$ ). Create a network flow instance as follows: create a network with a source  $s$ ,

577 sink  $t$ , and a vertex for each domain type  $a_1, \dots, a_n, b_1, \dots, b_m$ . Connect the source  $s$  of the  
 578 network to each  $a_i$  with a capacity  $c(a_i)$  edge, and connect each  $b_j$  to  $t$  with a capacity  $c(b_j)$   
 579 edge. Add an edge of capacity  $\infty$  from  $a_i$  to  $b_j$  if  $\delta(a_i, b_j)$  is non-zero (i.e. if  $a_i$  bonds to  $b_j$ ).  
 580 The max-flow of this network is equal to the maximum possible bonds achievable by any  
 581 configuration for the given MFE input and, therefore, can be used to determine the solution  
 582 to MFE in polynomial time  $\mathcal{O}(|\Lambda|^3)$ . We add an additional  $\log |\mathcal{S}|$  factor to this run time to  
 583 account for arithmetic based on strand counts. ◀

584 **Complementary Binding.** Lastly, we show that Theorem 18 *requires promiscuous binding*  
 585 single-domain strands. First, we describe how this problem can be solved sequentially in  
 586 time  $\mathcal{O}(|\Lambda|)$ , then describe how to parallelize it:

587 ▶ **Theorem 21.** *MFE of domain-level strand systems with 1-domain strands and comple-*  
 588 *mentary binding is solvable in time  $\mathcal{O}(|\Lambda| \log |\mathcal{S}|)$ .*

589 **Proof.** Each strand with domain  $a$  can only bond with its codomain  $a^*$ . This means the  
 590 number of complexes for that domain type pair is the smaller of the two numbers, which  
 591 we write as  $\min(|a|, |a^*|)$ . We can then compute the binding strength times number of  
 592 complexes  $\delta(a, a^*) \min(|a|, |a^*|)$  to get the first term of the function  $\Delta G(s)$  for an MFE  
 593 secondary structure  $s$ . The number of removed complexes is also  $\min(|a|, |a^*|)$ , which we  
 594 can multiply by  $\Delta G^{\text{assoc}}$  to get the contribution of the second term. In total, we are making  
 595  $|\Lambda|$  comparisons, each of two numbers  $\leq |\mathcal{S}|$ . Then we are summing up  $|\Lambda|$  minima, and  
 596 returning it. We add a  $\log |\mathcal{S}|$  factor to the run time to account for the cost of arithmetic  
 597 operations. ◀

598 The next result shows that the algorithm from Theorem 21 can be parallelized to get an  
 599 NC algorithm. Hence, MFE of single-domain, complementary binding systems cannot be  
 600 P-hard unless NC=P, in turn implying that non-complementary binding, i.e. promiscuous, is  
 601 likely required for efficient (polynomial time) simulation of arbitrary sequential computations  
 602 (Theorem 18).

603 ▶ **Theorem 22.** *MFE of domain-level strand systems with 1-domain strands and comple-*  
 604 *mentary binding is in NC when encoded in unary.*

605 **Proof.** For NC membership, we require, at most, polylogarithmic time on a polynomial  
 606 number of processors. The algorithm from Theorem 21 can be parallelized by computing  
 607 the smaller value between domains and codomains on  $|\Lambda|$  different processors. This can be  
 608 done in  $\mathcal{O}(\log |\mathcal{S}|)$  time. Then, we add the free energy contributions of each domain pair in  
 609 parallel, taking  $\mathcal{O}(\log |\Lambda| \log |\mathcal{S}|)$  parallel time in total. ◀

### 610 5.3 Counting Free Energy

611 The counting problem #FE is still hard, which we establish below. We show that there  
 612 exists a parsimonious reduction from counting matchings to #FE.

613 ▶ **Theorem 23.** *Counting the number of structures with energy  $E$  is #P-Complete even with*  
 614 *bipartite unit strength binding and encoded in unary.*

615 **Proof.** We reduce from Bipartite Matching. For each vertex, we create a domain  $v$ . For each  
 616 edge, we make the binding strength of both domains equal to  $-1$ . The set of configurations  
 617 of bonds is equivalent to the sets of edges. The energy of each configuration is a function  
 618 of the number of edges represented. Thus, if we can compute the number of configurations  
 619 with energy level  $E$  in polynomial time, we then determine the number of matchings. ◀

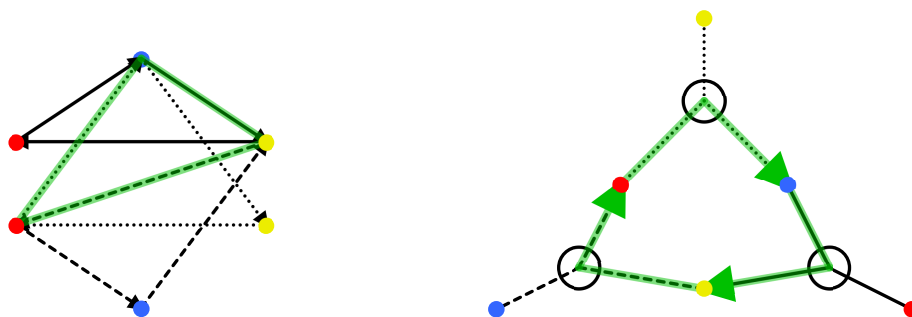


## References

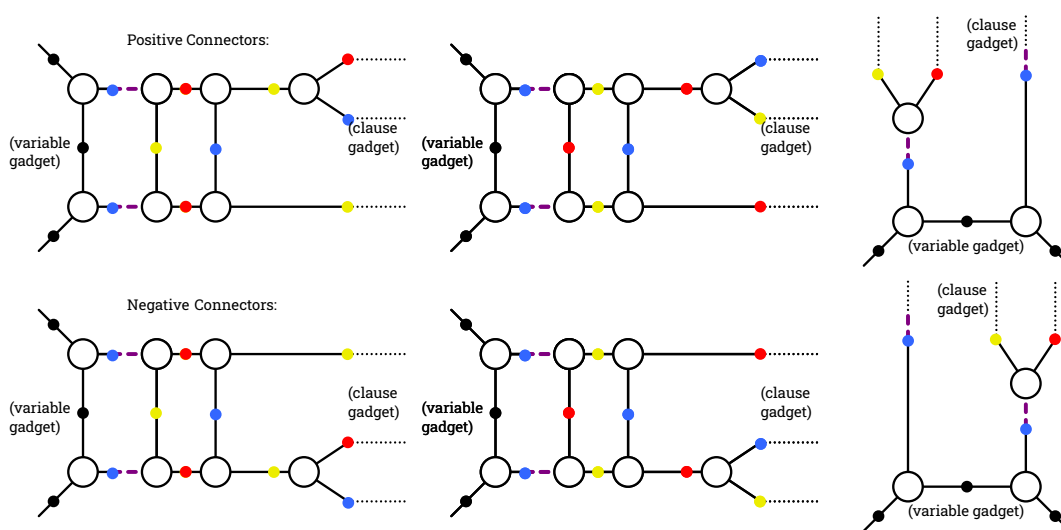
- 620 ———
- 621 1 Tatsuya Akutsu. Dynamic programming algorithms for RNA secondary structure prediction  
622 with pseudoknots. *Discrete Applied Mathematics*, 104(1-3):45–62, 2000.
- 623 2 Sanjeev Arora and Boaz Barak. *Computational complexity: a modern approach*. Cambridge  
624 University Press, 2009.
- 625 3 Nikhil Bansal, Tim Oosterwijk, Tjark Vredeveld, and Ruben Van Der Zwaan. Approximating  
626 vector scheduling: almost matching upper and lower bounds. *Algorithmica*, 76:1077–1096,  
627 2016.
- 628 4 Robert D Barish, Rebecca Schulman, Paul WK Rothmund, and Erik Winfree. An information-  
629 bearing seed for nucleating algorithmic self-assembly. *Proceedings of the National Academy of  
630 Sciences*, 106(15):6054–6059, 2009.
- 631 5 David A Mix Barrington, Neil Immerman, and Howard Straubing. On uniformity within  $NC^1$ .  
632 *Journal of Computer and System Sciences*, 41(3):274–306, 1990.
- 633 6 Alexander Barvinok and Alex Samorodnitsky. Computing the partition function for perfect  
634 matchings in a hypergraph. *Combinatorics, Probability and Computing*, 20(6):815–835, 2011.
- 635 7 Kimon Boehmer, Sarah J Berkemer, Sebastian Will, and Yann Ponty. Rna triplet repeats:  
636 Improved algorithms for structure prediction and interactions. 2024. 24th Workshop on  
637 Algorithms in Bioinformatics (WABI), to appear.
- 638 8 Richard A Brualdi. *Introductory combinatorics*. Pearson Education India, 1977.
- 639 9 Andrei Bulatov and Martin Grohe. The complexity of partition functions. *Theoretical Computer  
640 Science*, 348(2):148–186, 2005. Automata, Languages and Programming: Algorithms and  
641 Complexity (ICALP-A 2004).
- 642 10 Luca Cardelli. Two-domain DNA strand displacement. *Mathematical Structures in Computer  
643 Science*, 23(2):247–271, 2013.
- 644 11 Ho-Lin Chen, Anne Condon, and Hosna Jabbari. An  $O(n^5)$  algorithm for MFE prediction of  
645 kissing hairpins and 4-chains in nucleic acids. *Journal of Computational Biology*, 16(6):803–815,  
646 2009.
- 647 12 Anne Condon, Monir Hajiaghayi, and Chris Thachuk. Predicting Minimum Free Energy  
648 Structures of Multi-Stranded Nucleic Acid Complexes Is APX-Hard. In Matthew R. Lakin  
649 and Petr Šulc, editors, *27th International Conference on DNA Computing and Molecular  
650 Programming (DNA 27)*, volume 205 of *Leibniz International Proceedings in Informatics  
651 (LIPIcs)*, pages 9:1–9:21, Dagstuhl, Germany, 2021. Schloss Dagstuhl – Leibniz-Zentrum für  
652 Informatik.
- 653 13 Robert M Dirks, Justin S Bois, Joseph M Schaeffer, Erik Winfree, and Niles A Pierce.  
654 Thermodynamic analysis of interacting nucleic acid strands. *SIAM review*, 49(1):65–88, 2007.
- 655 14 Robert M Dirks and Niles A Pierce. A partition function algorithm for nucleic acid secondary  
656 structure including pseudoknots. *Journal of computational chemistry*, 24(13):1664–1677, 2003.
- 657 15 Robert M Dirks and Niles A Pierce. An algorithm for computing nucleic acid base-pairing  
658 probabilities including pseudoknots. *Journal of computational chemistry*, 25(10):1295–1304,  
659 2004.
- 660 16 David Doty, Trent A Rogers, David Soloveichik, Chris Thachuk, and Damien Woods. Thermo-  
661 dynamic binding networks. In *DNA23: The 23rd International Conference on DNA Computing  
662 and Molecular Programming*, volume 10467 of *LNCS*, pages 249–266. Springer, 2017.
- 663 17 Martin E. Dyer and Alan M. Frieze. Planar 3DM is NP-Complete. *J. Algorithms*, 7(2):174–184,  
664 1986.
- 665 18 Constantine G. Evans. *Crystals that count! Physical principles and experimental investigations  
666 of DNA tile self-assembly*. PhD thesis, Caltech, 2014.
- 667 19 Constantine G Evans, Jackson O’Brien, Erik Winfree, and Arvind Murugan. Pattern recogni-  
668 tion in the nucleation kinetics of non-equilibrium self-assembly. *Nature*, 625(7995):500–507,  
669 2024.
- 670 20 M. R. Garey and David S. Johnson. *Computers and Intractability: A Guide to the Theory of  
671 NP-Completeness*. W. H. Freeman, 1979.

- 672 21 Michael R Garey and David S Johnson. “strong” NP-completeness results: Motivation,  
673 examples, and implications. *Journal of the ACM (JACM)*, 25(3):499–508, 1978.
- 674 22 Cody Geary, Paul WK Rothemund, and Ebbe S Andersen. A single-stranded architecture for  
675 cotranscriptional folding of RNA nanostructures. *Science*, 345(6198):799–804, 2014.
- 676 23 Leslie M Goldschlager. The monotone and planar circuit value problems are LOG SPACE  
677 complete for P. *ACM SIGACT news*, 9(2):25–29, 1977.
- 678 24 Raymond Greenlaw, H James Hoover, and Walter L Ruzzo. *Limits to parallel computation:  
679 P-completeness theory*. Oxford University Press, USA, 1995.
- 680 25 Ivo L Hofacker, Christian M Reidys, and Peter F Stadler. Symmetric circular matchings and  
681 RNA folding. *Discrete mathematics*, 312(1):100–112, 2012.
- 682 26 Russell Impagliazzo, Ramamohan Paturi, and Francis Zane. Which Problems Have Strongly  
683 Exponential Complexity? *J. Comput. Syst. Sci.*, 63(4):512–530, 2001.
- 684 27 Hosna Jabbari, Ian Wark, Carlo Montemagno, and Sebastian Will. Knotty: efficient and  
685 accurate prediction of complex RNA pseudoknot structures. *Bioinformatics*, 34(22):3849–3856,  
686 2018.
- 687 28 Ronny Lorenz, Stephan H Bernhart, Christian Höner zu Siederdissen, Hakim Tafer, Christoph  
688 Flamm, Peter F Stadler, and Ivo L Hofacker. ViennaRNA package 2.0. *Algorithms for  
689 molecular biology*, 6:1–14, 2011.
- 690 29 Rune B Lyngsø and Christian NS Pedersen. Pseudoknots in RNA secondary structures. In  
691 *Proceedings of the fourth annual international conference on Computational molecular biology*,  
692 pages 201–209, 2000.
- 693 30 Rune B Lyngsø and Christian NS Pedersen. RNA pseudoknot prediction in energy-based  
694 models. *Journal of computational biology*, 7(3-4):409–427, 2000.
- 695 31 Rune B Lyngsø, Michael Zuker, and CN Pedersen. Fast evaluation of internal loops in RNA  
696 secondary structure prediction. *Bioinformatics (Oxford, England)*, 15(6):440–445, 1999.
- 697 32 John S McCaskill. The equilibrium partition function and base pair binding probabilities for  
698 RNA secondary structure. *Biopolymers: Original Research on Biomolecules*, 29(6-7):1105–1119,  
699 1990.
- 700 33 Cristopher Moore and Stephan Mertens. *The Nature of Computation*. Oxford University Press,  
701 2011.
- 702 34 Cristopher Moore and Stephan Mertens. *The Nature of Computation*. Oxford University Press,  
703 2011.
- 704 35 Maxim P Nikitin. Non-complementary strand commutation as a fundamental alternative for  
705 information processing by DNA and gene regulation. *Nature Chemistry*, 15(1):70–82, 2023.
- 706 36 Ruth Nussinov and Ann B Jacobson. Fast algorithm for predicting the secondary structure of  
707 single-stranded RNA. *Proceedings of the National Academy of Sciences*, 77(11):6309–6313,  
708 1980.
- 709 37 Lulu Qian and Erik Winfree. Scaling up digital circuit computation with DNA strand  
710 displacement cascades. *Science*, 332(6034):1196–1201, 2011.
- 711 38 Jens Reeder and Robert Giegerich. Design, implementation and evaluation of a practical  
712 pseudoknot folding algorithm based on thermodynamics. *BMC bioinformatics*, 5:1–12, 2004.
- 713 39 Elena Rivas and Sean R Eddy. A dynamic programming algorithm for RNA structure prediction  
714 including pseudoknots. *Journal of molecular biology*, 285(5):2053–2068, 1999.
- 715 40 Paul WK Rothemund. Folding DNA to create nanoscale shapes and patterns. *Nature*,  
716 440(7082):297–302, 2006.
- 717 41 John SantaLucia Jr and Donald Hicks. The thermodynamics of DNA structural motifs. *Annu.  
718 Rev. Biophys. Biomol. Struct.*, 33:415–440, 2004.
- 719 42 Thomas J. Schaefer. The Complexity of Satisfiability Problems. In Richard J. Lipton, Walter A.  
720 Burkhard, Walter J. Savitch, Emily P. Friedman, and Alfred V. Aho, editors, *Proceedings  
721 of the 10th Annual ACM Symposium on Theory of Computing, May 1-3, 1978, San Diego,  
722 California, USA*, pages 216–226. ACM, 1978.

- 723 43 Rebecca Schulman and Erik Winfree. Synthesis of crystals with a programmable kinetic barrier  
724 to nucleation. *Proceedings of the National Academy of Sciences*, 104(39):15236–15241, 2007.
- 725 44 Ahmed Shalaby, Chris Thachuk, and Damien Woods. Minimum free energy, partition function  
726 and kinetics simulation algorithms for a multistranded scaffolded DNA computer. In Ho-Lin  
727 Chen and Constantine G. Evans, editors, *29th International Conference on DNA Computing  
728 and Molecular Programming (DNA 29)*, volume 276 of *Leibniz International Proceedings in  
729 Informatics (LIPIcs)*, pages 1:1–1:22, Dagstuhl, Germany, 2023. Schloss Dagstuhl–Leibniz-  
730 Zentrum für Informatik.
- 731 45 Ahmed Shalaby and Damien Woods. An efficient algorithm to compute the minimum free  
732 energy of interacting nucleic acid strands, 2024. Arxiv preprint: [arXiv:2407.09676](https://arxiv.org/abs/2407.09676).
- 733 46 Friedrich C Simmel, Bernard Yurke, and Hari R Singh. Principles and applications of nucleic  
734 acid strand displacement reactions. *Chemical reviews*, 119(10):6326–6369, 2019.
- 735 47 David Soloveichik, Georg Seelig, and Erik Winfree. DNA as a universal substrate for chemical  
736 kinetics. *Proceedings of the National Academy of Sciences*, 107(12):5393–5398, 2010.
- 737 48 Niranjana Srinivas, James Parkin, Georg Seelig, Erik Winfree, and David Soloveichik. Enzyme-  
738 free nucleic acid dynamical systems. *Science*, 358(6369):eaal2052, 2017.
- 739 49 Yasuo Uemura, Aki Hasegawa, Satoshi Kobayashi, and Takashi Yokomori. Tree adjoining  
740 grammars for RNA structure prediction. *Theoretical computer science*, 210(2):277–303, 1999.
- 741 50 Klaus W Wagner. The complexity of combinatorial problems with succinct input representation.  
742 *Acta informatica*, 23:325–356, 1986.
- 743 51 Boya Wang, Chris Thachuk, Andrew D Ellington, Erik Winfree, and David Soloveichik.  
744 Effective design principles for leakless strand displacement systems. *Proceedings of the National  
745 Academy of Sciences*, 115(52):E12182–E12191, 2018.
- 746 52 Bryan Wei, Mingjie Dai, and Peng Yin. Complex shapes self-assembled from single-stranded  
747 DNA tiles. *Nature*, 485(7400):623–626, 2012.
- 748 53 Erik Winfree, Furong Liu, Lisa A Wenzler, and Nadrian C Seeman. Design and self-assembly  
749 of two-dimensional DNA crystals. *Nature*, 394(6693):539–544, 1998.
- 750 54 Damien Woods, David Doty, Cameron Myhrvold, Joy Hui, Felix Zhou, Peng Yin, and Erik  
751 Winfree. Diverse and robust molecular algorithms using reprogrammable DNA self-assembly.  
752 *Nature*, 567(7748):366–372, 2019.
- 753 55 David Yu Zhang and Georg Seelig. Dynamic DNA nanotechnology using strand-displacement  
754 reactions. *Nature chemistry*, 3(2):103–113, 2011.
- 755 56 Michael Zuker and Patrick Stiegler. Optimal computer folding of large RNA sequences using  
756 thermodynamics and auxiliary information. *Nucleic acids research*, 9(1):133–148, 1981.



■ **Figure 5** (Left): Interleaving of three different (solid, dotted, dashed) directed 3-cycles could cause a new 3-cycle that is not among the given ones. (Right): Such a 3-cycle required a non-subdivided, triangular face formed from all three colors of the 3-cycles, not occurring in the reduction (Figure 7).



■ **Figure 6** All positive and negative connectors of the reduction in Figure 7.

757 **A Directed 3-Cycle Cover**

758 We reduce from directed 3-cycle cover, disallowing pairs of vertices with both edges between them, which we show is NP-hard in the following result. This result is inspired by problem [20,  
 759 GT11: Partition Into Triangles], but generalized to directed graphs. We require an additional  
 760 constraint as well, that there do not exist any two cycles in our graph.  
 761

762 A 3-cycle cover has exactly  $\frac{n}{3}$  cycles, so we must design our reduction to have exactly  
 763 that number of complexes in the minimum free energy structure. To address this, we must  
 764 make sure that complexes representing 3-cycles are the smallest cycles in our system. This is  
 765 true if our graph does not contain any 2-cycles, which requires that the graph not contain  
 766 any doubly covered edges. We now prove NP-hardness and some technical lemmas for our  
 767 reduction, with variable  $n$  denoting the number of vertices in the graph and  $m$  denoting the  
 768 number of edges.

769 ► **Theorem 24.** *Directed 3-Cycle Cover is NP-hard even on graphs without any 2-cycles.*

770 **Proof.** Planar 3DM [17] is NP-hard even when there are no faces of size 3 without a set. It  
 771 turns out that mimicking the reduction by Dyer and Frieze is enough. Indeed, this reduction

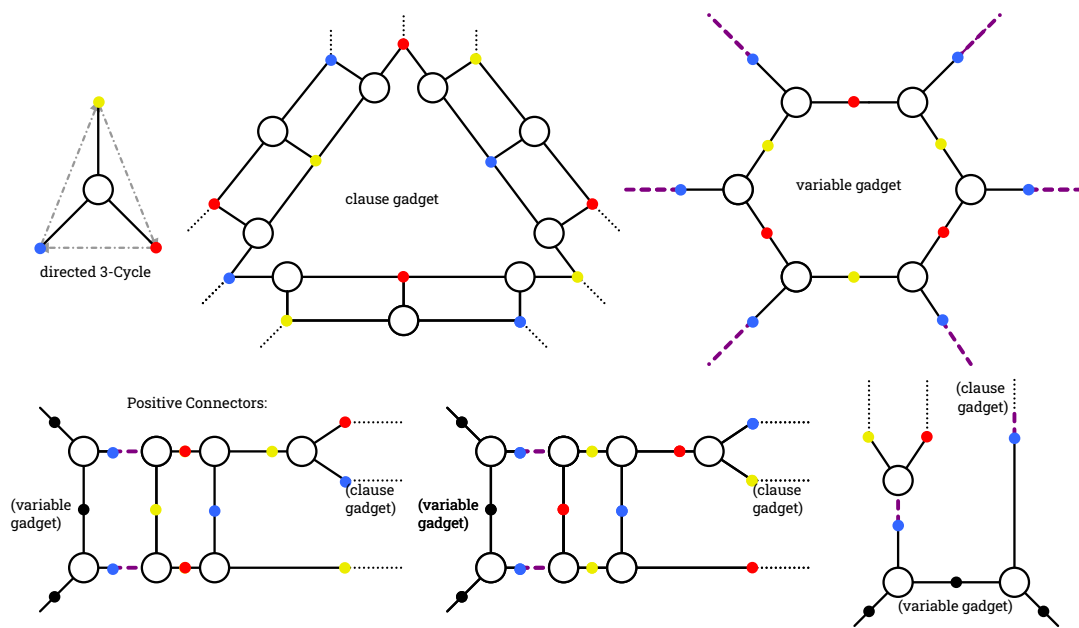


**Figure 7** Reduction from 1-in-3SAT to Directed 3-Cycle Cover, which borrows from the reduction to 3DM [17]. (Top): Notation of directed 3-cycles, as well as clause gadgets and variable gadgets. (Bottom): Connectors from positive variable appearances to the clause gadgets. Negative connectors are obtained by swapping the branches going into the clause gadget (see Figure 6 for details). Correctness follows from [17] and the observation of two properties. See the proof of Theorem 24.

772 does not require planarity but rather preserves it, i.e., the gadgets still work in the non-planar  
 773 setting. We summarize their gadgets in Figure 7. Their gadgets are taken as is and use  
 774 colors to specify directed edges, which are fixed from blue to yellow, yellow to red, and red to  
 775 blue. The main observations we obtain from these gadgets are that (1) there is no 2-cycle in  
 776 the reduction and (2) there is no new 3-cycle that is not given but can be constructed from  
 777 a combination of given 3-cycles. Indeed, (1) can't occur as we only construct directed edges  
 778 from vertices of color blue to yellow, yellow to red, and red to blue. So, the corresponding  
 779 inverse edge can never exist. The only possibility for (2) is depicted in Figure 5 (left), which  
 780 would be the case if we combined three different 3-cycles. However, to address this, we  
 781 require each face uses three differently colored nodes (see Figure 5 (right)), which is not  
 782 possible in [17] (see also Figure 7). ◀

783 ▶ **Lemma 25.** *Every 3-cycle cover algorithm on directed graphs with  $n$  vertices, even on*  
 784 *graphs which do not contain any 2-cycles, has a runtime  $2^{\Omega(n)}$  unless ETH fails.*

785 **Proof.** We first note that the reduction from 3SAT to 1-in-3SAT [42] only increases the  
 786 number of variables by a linear amount. We then track the chain of reductions from 1-in-  
 787 3SAT, to 3DM [17], to 3-Cycle cover (Thm. 24) and show the number of vertices in the cycle  
 788 cover graph is linear in the number of 1-in-3SAT variables, as we do require the reduction  
 789 to preserve planarity. This preserves the  $2^{\Omega(n)}$  lower bound under ETH [26] from SAT to  
 790 3-cycle cover. We also note that a  $2^{\Omega(n)}$  ETH lower bound for 3DM was shown in [3]. ◀

791 ▶ **Lemma 26.** *All secondary structures achieve at most  $2n$  bonds.*

792 **Proof.** Each bond in any secondary structure must include a domain from one of the vertex  
 793 species, and each species has 2 such domains, so the total number of bonds is at most  $2n$ . ◀

## 23:22 Domain-Based Nucleic-Acid Minimum Free Energy

794 ► **Lemma 27.** *A 3-cycle secondary structure (if it exists) has  $2n$  bonds and  $m - \frac{2n}{3}$  distinct*  
795 *complexes.*

796 **Proof.** Each domain of each vertex species is bonded to an edge species in a 3-cycle secondary  
797 structure, which implies the structure achieves  $2n$  bonds. For the number of distinct complexes,  
798 we can count them by including the number of cycles ( $\frac{n}{3}$ ) plus the number of remaining edge  
799 species. Since each cycle complex absorbs exactly 3 edge species, the number of remaining  
800 edge species is  $m - n$ , yielding a total of  $m - \frac{2n}{3}$  total distinct complexes. ◀

801 ► **Lemma 28.** *Any secondary structure with  $2n$  bonds that is not a 3-cycle secondary structure*  
802 *has less than  $m - \frac{2n}{3}$  distinct complexes.*

803 **Proof.** Consider a secondary structure of  $2n$  bonds that is not a 3-cycle secondary structure.  
804 Note that each vertex species must be bonded to exactly 2 edge species to achieve  $2n$  bonds.  
805 Let  $d + r$  denote the number of connected complexes in the structure that contain at least  
806 one vertex species, with  $r$  specifically denoting the number of such complexes that form a  
807 connected cycle, and  $d$  denoting the number of those that do not.

808 For each of the  $r$  complexes that form a closed cycle of bonds, the number of edge species  
809 included in the complex is the same as the number of vertices in the complex, whereas,  
810 for each of the  $d$  non-cycle complexes, the edge count is one more than the number of  
811 vertices in the cycle. Therefore, the total number of edge species that are bonded to one  
812 of these complexes is  $n + d$ . The total number of complexes in the secondary structure  
813 can be calculated by including the number of complexes that absorb the vertex species  
814 ( $d + r$ ) plus the number of remaining (unbonded) edge species ( $m - n - d$ ), for a total of  
815  $(d + r) + (m - n - d) = m - n + r$ . If this secondary structure is not a 3-cycle structure, then  
816  $r < \frac{n}{3}$ , and so this total is less than  $m - \frac{2n}{3}$ . ◀

817 ► **Lemma 29.** *If the associative free energy  $0 < \Delta G^{\text{assoc}} < 1$ , then the minimum free energy*  
818 *secondary structure has  $2n$  bonds.*

819 **Proof.** Any secondary structure with fewer than  $2n$  bonds would have two separate complexes  
820 with complementary, unbonded domains. A new configuration could, therefore, be constructed  
821 by combining these two complexes through this pair of domains and increasing both the  
822 bond count and complex count by 1. Since  $\Delta G^{\text{assoc}} < 1$ , this new secondary structure would  
823 have less free energy than the original structure, implying only a maximal  $2n$  bond secondary  
824 structure could be the minimum energy structure. ◀

825

**B Additional Figures**

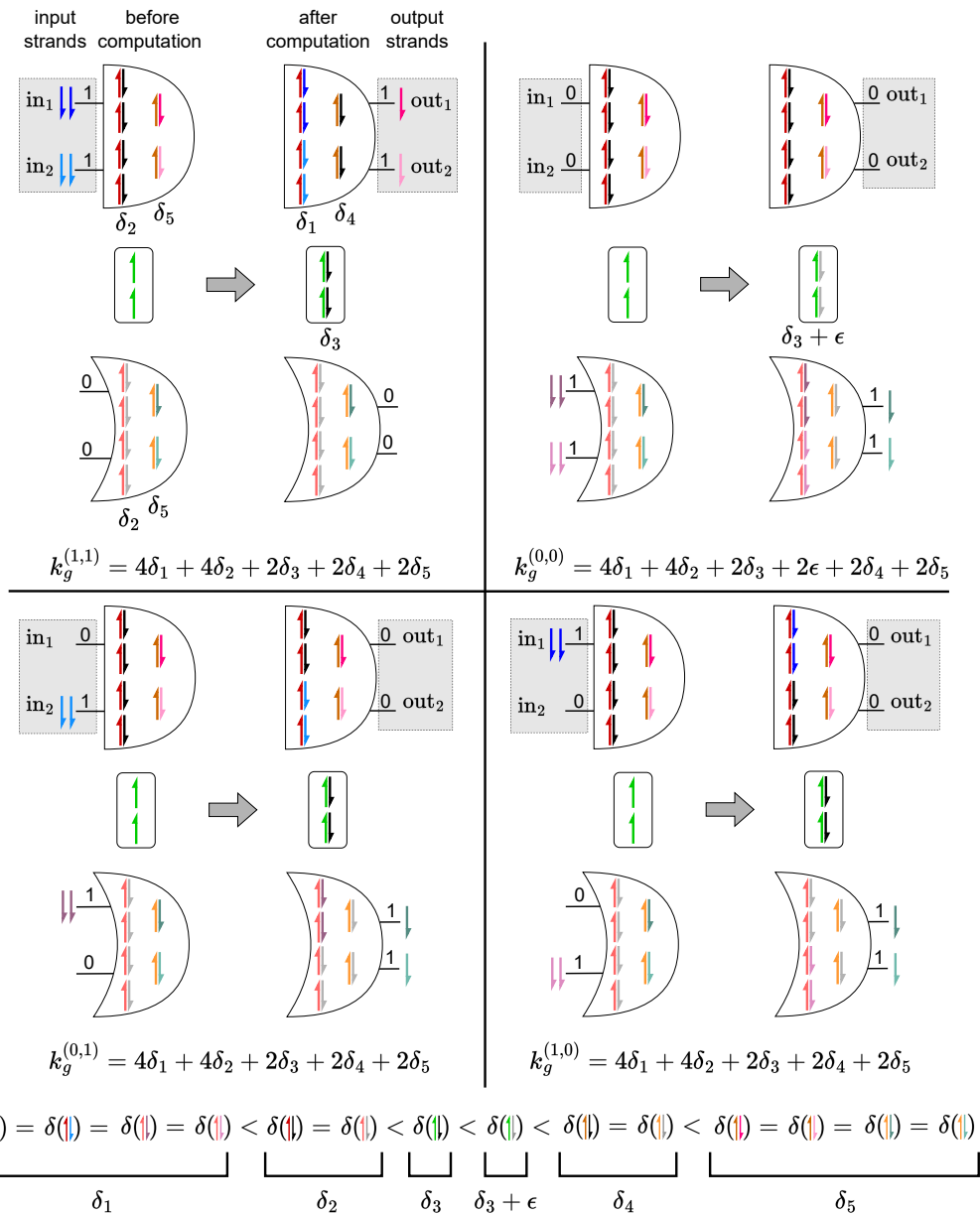
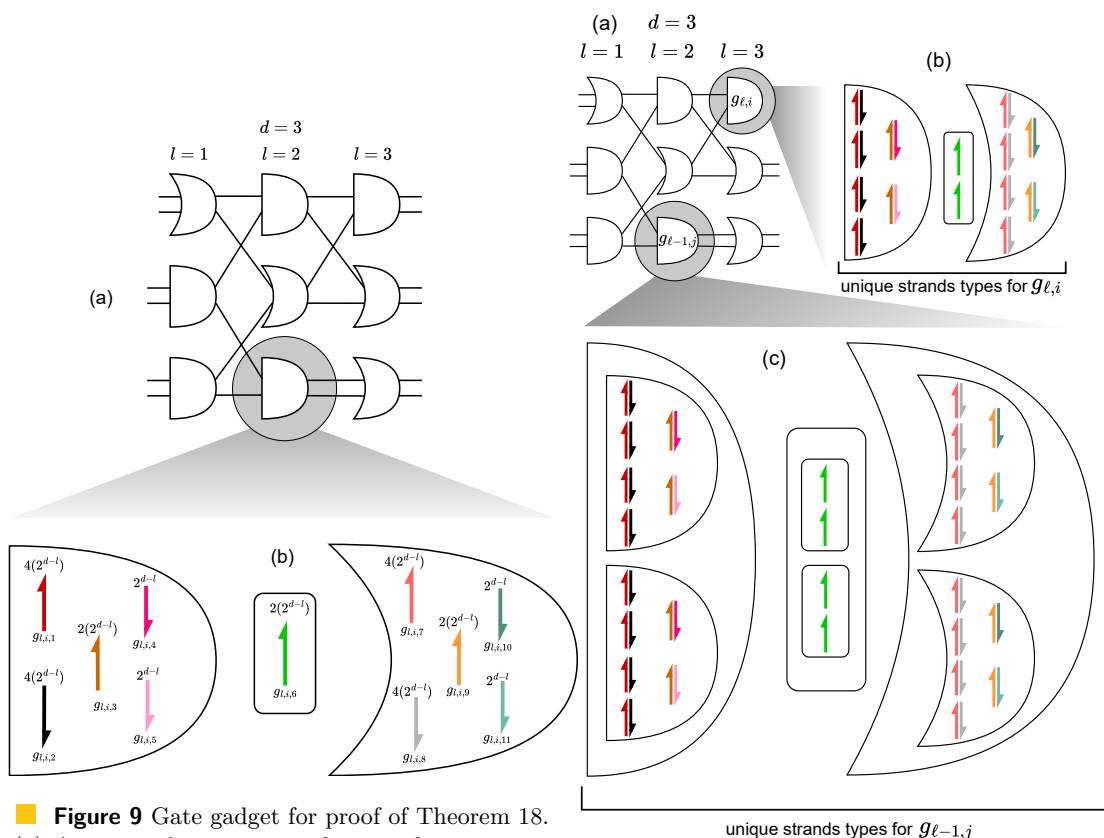


**Figure 8** Gate gadget for proof of Theorem 18, showing the design for simulating a circuit consisting of a single AND gate (i.e. depth 1). Simulation of a single AND gate with input bits  $in_1, in_2 \in \{0, 1\}$  and output bits  $out_1, out_2 \in \{0, 1\}$ . Panels in row-major order respectively show input bit pair 11, 00, 01, and 10. Intuitively, the gadget simulates AND in a dual-rail fashion using three components: an AND component, plus two components that work together to act as a dual to the AND: a small intermediate component (green strands) and an OR component. Together, with a dual rail encoding of the input bits, the three components work to keep the gate energy ( $\Delta G()$ ) almost constant (i.e. constant up to  $-\epsilon$ ). To simulate an OR gate, the same gadget is used, except that inputs are flipped, and the output comes from the OR instead of the AND component.  $k_g^{(x,y)}$  denotes the MFE of gate  $g$  with input  $(x, y)$ .



■ **Figure 9** Gate gadget for proof of Theorem 18. (a) An example monotone, fanin-2, fanout-2 circuit  $C$ , with a  $3 \times 3$  layout of AND and OR gates. (b) Design for an arbitrary strand gadget simulating the highlighted AND gate  $g_{\ell,i}$  (the  $i$ th gate at layer  $\ell$  in  $C$ ). This gate gadget has 11 strand types named  $g_{\ell,i,1}$  to  $g_{\ell,i,11}$  that are unique to that gate gadget (they appear in no other gate gadget), with the counts of each strand type shown directly above, as a superscript to the strand type.

■ **Figure 10** Recursive nature of the construction in the proof of Theorem 18. (a) An example monotone, fanin-2, fanout-2 circuit  $C$ , with a  $3 \times 3$  layout of AND and OR gates. (b) Design for the strand gadget simulating the highlighted AND gate  $g_{\ell,i}$  at the output layer. (c) Design the strand gadget simulating the highlighted AND gate  $g_{\ell-1,j}$  in the layer just before the output layer. Note that the 11 strand types in each outlined gate gadget are unique to that outlined gate gadget, despite colour-repetition between gadgets  $g_{\ell,i}$  and  $g_{\ell-1,j}$ .